

AD-A064 546

CALIFORNIA UNIV BERKELEY DEPT OF PHYSICS  
NUMERICAL ANALYSIS OF WEAKLY NONLINEAR WAVE TURBULENCE (HAMILTO--ETC(U)  
JAN 79 J D MEISS, N POMPHREY, K M WATSON N00014-78-C-0050  
UCB-PTH-79/2 NL

F/G 20/4

UNCLASSIFIED

| OF |  
AD  
AO 64546




END  
DATE  
FILMED

4 -- 79  
DDC

LEVEL II (12)

14 UCB-PTH-79/2

11 Jan 1979

ADA064546

6 NUMERICAL ANALYSIS OF WEAKLY NONLINEAR WAVE TURBULENCE  
(Hamilton's Principle, Wave-Wave Interactions,  
Oceanic Internal Waves, Relaxation Phenomena,  
Statistical Mechanics),

15 N00014-78-C-0050<sup>new</sup>

10 James D./Meiss,  
Neil/Pomphrey  
and  
Kenneth M/Watson

12 33p.

Department of Physics  
and  
Lawrence Berkeley Laboratory  
University of California  
Berkeley, California 94720

DDC  
RECEIVED  
FEB 18 1979  
E

ACCESSION for	
NTIS	White Section <input checked="" type="checkbox"/>
DDC	Buff Section <input type="checkbox"/>
UNANNOUNCED	<input type="checkbox"/>
JUSTIFICATION	per DDC Form 50
BY	
DISTRIBUTION/AVAILABILITY CODES	
Dist.	Avail. and/or Special
A	

Abstract

This paper studies the propagation of weakly nonlinear waves. The analysis is applicable to plasma waves, surface water waves, the interaction of laser beams with matter, particle accelerators, etc. The specific motivation for this work is, however, the study of internal waves in the ocean. Hamilton's principle is used to write the fluid equations in Hamiltonian form in terms of linear eigenmode amplitudes. Numerical studies are made of the effect of Fourier grid size and resonance widths. Statistical information is generated from an ensemble of initial states of the random wave field.

DDC FILE COPY

79 02 09 080

071970 B

## 1. Introduction

In this paper we consider some techniques used to study statistical properties of weak turbulence associated with nonlinear wave-wave interactions. Specifically, we apply the analysis to buoyancy dominated turbulence of internal waves in the ocean. Stable stratification, a characteristic of the oceans, implies an equilibrium depth about which each fluid element oscillates. The resulting "almost two-dimensional" system avoids some of the complexity of fully three-dimensional weak turbulence.

Formally, our wave system corresponds to a set of harmonic oscillators with weakly nonlinear couplings. Similar dynamical systems are encountered in the study of surface water waves (1), plasma waves (2), the interaction of light with matter, particle accelerators, etc. Interest in the properties of oscillators with weakly non-linear couplings has been stimulated by the KAM theorem (3), the discovery of solitons (4) and other studies (5).

Relaxation phenomena associated with linearly coupled oscillators have been studied by Mazur and Montroll (6) and by Ford, Kac and Mazur (7). Computations with a linear chain of fifty oscillators by Cukier, Shuler, and Weeks (8) have shown agreement with the predictions of a Langevin model for the system.

Weakly nonlinear oscillator systems have been studied by several statistical models. Use of random phase and two-time scale approximations allows termination of a sequence of coupled moment equations to give a Boltzmann-type transport equation. This approach has been used by Hasselman

(9) for geophysical phenomena, Snider (10) for gas kinetic theory and Davidson (2) for plasmas. The technique of Prigogine and collaborators (11) of simplifying the Liouville equation by the neglect of higher order correlations also leads to the Boltzmann transport equation. In a future publication we will show how the fluctuation-dissipation theorem (12) and the Krylov-Bogoliubov-Mitropolsky two-time perturbation method (13,14) can be used to obtain Langevin and Fokker-Planck descriptions of internal wave turbulence.

These models can be compared with numerical solutions of the equations of motion, providing evidence for the validity of the approximations used. The ocean internal wave system lends itself particularly well to numerical computation because of the "almost two-dimensional" nature of the equations. Recently, the Hasselman transport theory has been applied to this system by McComas and Bretherton (15) and Olbers (16). These studies utilize the remarkable synthesis of experimental observations, made by Garrett and Munk (17,18), who proposed an explicit equilibrium spectrum.

In this paper an explicit Hamiltonian is given which describes the nonlinear transfer of energy among the linear eigenmodes of the internal wave field. A "test wave" model is developed which can be used to compare numerical results with statistical models. This model describes the propagation of a single, labeled wave through an ambient medium. Computational methods for integration of Hamilton's equations are also discussed.

79 02 09 080

## 2. Dynamical Formulation of the Wave Interactions

We consider as a model a "plane" ocean of uniform depth and having rectangular area  $\Sigma_0$ . Periodic boundary conditions are used at the sides, and the top and bottom surfaces are assumed rigid. The quiescent upper surface coincides with the plane  $z = 0$  of a rectangular coordinate system. The bottom is at  $z = -H$ . The equilibrium fluid density is  $\rho(z)$ , a monotonically increasing function of depth. The quantity

$$N(z) = \left[ -\frac{g}{\rho} \frac{d\rho}{dz} \right]^{1/2} \quad [2.1]$$

is the Väisälä, or buoyancy frequency ( $g$  is the acceleration due to gravity). The fluid is incompressible and inviscid.

We introduce a Lagrangian and use Hamilton's principle to obtain the equations of fluid motion. The Lagrange coordinate of a fluid particle at time  $t$  is  $\underline{Y}(\underline{r}, t)$ , where  $\underline{r} = \underline{Y}(\underline{r}, 0)$  is its position at  $t = 0$ . The appropriate Lagrangian per unit area is (20)

$$L = \int \frac{d^3r}{\Sigma_0} \left( \frac{1}{2} \rho |\dot{\underline{Y}}|^2 + \rho \underline{g} \cdot \underline{Y} - \frac{1}{2} \rho \underline{f} \cdot (\dot{\underline{Y}} \times \underline{Y}) + P(\underline{r}) \left[ J \left( \frac{\partial \underline{Y}}{\partial \underline{r}} \right) - 1 \right] \right) . \quad [2.2]$$

The first three terms in the integrand represent, respectively, kinetic energy, negative of gravitational potential energy, and rotational energy due to Coriolis coupling. The quantity "f" is twice the angular frequency of the earth's rotation. The final term expresses the constraint due to

incompressibility:  $P$  is a Lagrange multiplier and  $J$  is the Jacobian of the transformation  $\underline{r} \rightarrow \underline{Y}$ .

Hamilton's principle states that the functional

$$I = \int_{t_1}^{t_2} L dt \quad [2.3]$$

is stationary with respect to arbitrary independent variations in  $\underline{Y}$  and  $P$ , which vanish at  $t_1$  and  $t_2$  and at the boundaries of the fluid. In particular, variation of  $P$  yields the incompressibility condition

$$J \left( \frac{\partial \underline{Y}}{\partial \underline{r}} \right) = 1, \quad [2.4]$$

and variation of  $\underline{Y}$  yields the equations of motion

$$\rho \ddot{\underline{Y}} - \rho \underline{g} + \rho \underline{f} \times \dot{\underline{Y}} + \frac{\partial}{\partial \underline{Y}} P = 0 \quad [2.5]$$

The Lagrange multiplier  $P$  can therefore be identified with the fluid pressure. It may be considered a function of  $\underline{Y}$  and  $t$  in the Lagrangian since this adds terms with zero variation.

Rather than use [2.4] and [2.5] directly, we develop a perturbation-variation approach with the aim of obtaining a Hamiltonian which describes the lowest order nonlinear internal wave motions. Following Bretherton and Garrett (19), we define the displacement

$$\underline{\xi}(\underline{r}, t) \equiv \underline{Y}(\underline{r}, t) - \underline{r} \quad [2.6]$$

and consider  $|\underline{\xi}|$  to be a small quantity. The Lagrange multiplier  $P$  may then be expanded as

$$P(\underline{Y}, t) = P(\underline{r}, t) + (\underline{\xi} \cdot \underline{\nabla})P(\underline{r}, t) + \frac{1}{2} (\xi_i \xi_j \nabla_i \nabla_j)P(\underline{r}, t) + \dots \quad [2.7]$$

Substitution into [2.2] yields

$$L = \int \frac{d^3 \underline{r}}{\Sigma_0} \left[ \frac{1}{2} \rho |\dot{\underline{\xi}}|^2 + \rho \underline{g} \cdot \underline{\xi} - \frac{1}{2} \rho \underline{f} \cdot (\underline{\xi} \times \underline{\xi}) \right. \\ \left. - (\underline{\xi} \cdot \underline{\nabla})P(\underline{r}, t) - \frac{1}{2} (\xi_i \xi_j \nabla_i \nabla_j)P(\underline{r}, t) + \dots \right] , \quad [2.8]$$

where we have used the relation

$$\int d^3 \underline{r} P(\underline{Y}, t) J(\partial \underline{Y} / \partial \underline{r}) = \int d^3 \underline{Y} P(\underline{Y}, t) = \int d^3 \underline{r} P(\underline{r}, t) ,$$

and omitted terms independent of  $\underline{\xi}$ .

Next, we define the pressure fluctuation

$$\pi(\underline{r}, t) \equiv P(\underline{r}, t) - P(\underline{r}) \quad [2.9]$$

and assume it is a small quantity of the same order as  $|\underline{\xi}|$ . On introducing [2.9] into [2.8] and collecting terms, we obtain

$$L = L_1 + L_2 + L_3 + \dots ,$$

$$L_1 = \int \frac{d^3r}{\Sigma_0} [\rho \underline{g} \cdot \underline{\xi} - (\underline{\xi} \cdot \underline{\nabla}) P(r)] ,$$

$$L_2 = \int \frac{d^3r}{\Sigma_0} \left[ \frac{1}{2} \rho |\dot{\underline{\xi}}|^2 - \frac{\rho}{2} \underline{f} \cdot (\dot{\underline{\xi}} \times \underline{\xi}) - (\underline{\xi} \cdot \underline{\nabla}) \pi - \frac{1}{2} (\xi_i \xi_j \nabla_i \nabla_j) P(r) \right] ,$$

$$L_3 = \int \frac{d^3r}{\Sigma_0} \left[ -\frac{1}{2} (\xi_i \xi_j \nabla_i \nabla_j) \pi - \frac{1}{6} (\xi_i \xi_j \xi_k \nabla_i \nabla_j \nabla_k) P(r) \right] . \quad [2.10]$$

The equations of motion in each order are obtained by variation of

$$I_j = \int_{t_1}^{t_2} L_j dt$$

with respect to  $\underline{\xi}$  and  $\pi$ . Variation of  $I_1$  with respect to  $\underline{\xi}$  gives

$$\rho \underline{g} = \underline{\nabla} P(r) . \quad [2.11]$$

Thus  $P$  is a function only of  $z$  and is identified as the hydrostatic pressure.

We may use [2.11] in the Lagrangian to eliminate  $P$  and ignore  $I_1$  from now on. Then

$$L = L_2 + L_3 + \dots ,$$

$$L_2 = \int \frac{d^3r}{\Sigma_0} \left[ \frac{1}{2} \rho |\dot{\underline{\xi}}|^2 - \frac{1}{2} \rho \underline{f} \cdot (\dot{\underline{\xi}} \times \underline{\xi}) - (\underline{\xi} \cdot \underline{\nabla}) \pi - \frac{1}{2} \rho N^2 \xi_3^2 \right] ,$$

$$L_3 = \int \frac{d^3r}{\Sigma_0} \left[ -\frac{1}{2} (\xi_i \xi_j \nabla_i \nabla_j) \pi - \frac{1}{2} \rho N^2 \xi_3^2 \nabla_3 \xi_3 \right] , \quad [2.12]$$



where  $N^2$  is defined by [2.1].

Linear equations of motion are obtained from variation of  $I_2$ :

$$\rho \ddot{\underline{\xi}} + \rho \underline{f} \times \dot{\underline{\xi}} + \nabla \pi + \rho N^2 \xi_3 \hat{z} = 0 \quad ,$$

$$\nabla \cdot \underline{\xi} = 0 \quad . \quad [2.13]$$

We now neglect the horizontal components of  $\underline{f}^*$ . This enables us to separate the horizontal and vertical parts of [2.13] and expand  $\xi_3(x, z, t)$  in the rectangular area  $\Sigma_0$  as<sup>†</sup>

$$\xi_3(x, z, t) = \sum_{\alpha=1}^{\infty} \sum_{\underline{k}} A_{\underline{k}\alpha}(t) W_{\underline{k}\alpha}(z) e^{i\underline{k} \cdot \underline{x}}$$

$$A_{-\underline{k}\alpha} = A_{\underline{k}\alpha}^* \quad [2.14]$$

(the first sum extends over all positive integers  $\alpha$ ). Our task will be to obtain an expression for the Lagrangian [2.12] in terms of the field amplitudes  $A_{\underline{k}\alpha}(t)$ .

Using the definition [2.14] and some straightforward algebra, equations [2.13] yield

---

\*See, for example, Ref. (1), p. 239.

<sup>†</sup>Henceforth all vectors with the exception of  $\underline{f}$  will be two-dimensional in the horizontal plane.

$$\nabla_3 \rho \nabla_3 W_{k\alpha} + \rho k^2 \left( \frac{N^2 - \omega_\alpha^2(k)}{\omega_\alpha^2(k) - f^2} \right) W_{k\alpha} = 0 ,$$

$$\omega_\alpha(k) > 0 ,$$

$$W_{k\alpha}(-H) = W_{k\alpha}(0) = 0 . \quad [2.15]$$

This is a Sturm-Liouville equation for the modefunctions  $W_{k\alpha}(z)$  and eigenvalues  $\omega_\alpha(k)$ . The orthogonality relations

$$\frac{1}{\rho_0} \int_{-H}^0 \rho [N^2(z) - f^2] W_{k\alpha} W_{k\beta} dz = \delta_{\alpha\beta} \quad [2.16]$$

are readily deduced from [2.15]. The quantity  $\rho_0$  may, for example, be chosen as  $\rho(0)$ . The Fourier amplitudes  $A_{k\alpha}$  satisfy the equation

$$\ddot{A}_{k\alpha} + \omega_\alpha^2(k) A_{k\alpha} = 0 . \quad [2.17]$$

The horizontal displacement  $\xi_h$  is expressed in the form

$$\xi_h(x, z, t) = \sum_{\alpha=1}^{\infty} \sum_k [i k A_{k\alpha} + (i k x f) B_{k\alpha}] \frac{1}{k^2} W'_{k\alpha} e^{i k \cdot x} \quad [2.18]$$

where  $\dot{B}_{k\alpha} = A_{k\alpha}$  and  $W' \equiv dW/dz$ . The pressure fluctuation is then

$$\pi = -\rho \sum_{\alpha=1}^{\infty} \sum_k (\dot{A}_{k\alpha} + f^2 A_{k\alpha}) \frac{1}{k^2} W'_{k\alpha} e^{i k \cdot x} . \quad [2.19]$$

Expansions [2.14], [2.18] and [2.19] may be introduced into the

expression [2.10] for  $L_2$  to give

$$L_2 = \frac{\rho_0}{2} \sum_{\alpha=1}^{\infty} \sum_{\underline{k}} \left[ \frac{1}{\omega_{\alpha}^2(\underline{k}) - r^2} (\dot{A}_{\underline{k}\alpha} \dot{A}_{-\underline{k}\alpha} - \omega_{\alpha}^2(\underline{k}) A_{\underline{k}\alpha} A_{-\underline{k}\alpha}) \right] . \quad [2.20]$$

To obtain the nonlinear equations, we first write

$$\begin{aligned} \underline{\xi} &= \epsilon \underline{\xi}_1 + \epsilon^2 \underline{\xi}_2 + \dots , \\ \underline{\pi} &= \epsilon \underline{\pi}_1 + \epsilon^2 \underline{\pi}_2 + \dots , \end{aligned} \quad [2.21]$$

where  $\underline{\xi}_1, \underline{\pi}_1$  are the fields given in the linear approximation by equations [2.14] through [2.19], and  $\epsilon$  is a small parameter. Now, because  $I_2$  is stationary for small variations about the solutions  $\underline{\xi}_1, \underline{\pi}_1$ , we have

$$\begin{aligned} I_2 &= \int L_2(\underline{\xi}, \underline{\pi}) dt = \epsilon^2 \int L_2(\underline{\xi}_1, \underline{\pi}_1) dt + O(\epsilon^4) . \\ I_3 &= \int L_3(\underline{\xi}, \underline{\pi}) dt = \epsilon^3 \int L_3(\underline{\xi}_1, \underline{\pi}_1) dt + O(\epsilon^4) . \end{aligned} \quad [2.22]$$

Thus, since we do not wish to obtain equations valid beyond the order of  $\epsilon^3$  we may use the linear expressions [2.14]-[2.19] in deriving  $L_2$  and  $L_3$ .

In particular, we may use [2.17] to eliminate time derivative terms from  $L_3$ . It is important to realize that the nonlinear fields will continue to be expressed in the form [2.14]-[2.19] except that [2.17] will be modified.

We wish to express our equations in Hamiltonian form. As described

in some detail by Meiss and Watson\* this can be conveniently done by replacing the Fourier amplitudes  $A_{k\alpha}$  by canonical action angle variables

$J_{k\alpha}, \theta_{k\alpha}$ :

$$A_{k\alpha} = \frac{i}{\sqrt{2\omega_{\alpha} e_{k\alpha}}} \left[ \sqrt{J_{k\alpha}} e^{-i\theta_{k\alpha}} - \sqrt{J_{-k\alpha}} e^{i\theta_{-k\alpha}} \right]$$

$$B_{k\alpha} = -\frac{1}{\sqrt{2\omega_{\alpha}^3 e_{k\alpha}}} \left[ \sqrt{J_{k\alpha}} e^{-i\theta_{k\alpha}} + \sqrt{J_{-k\alpha}} e^{i\theta_{-k\alpha}} \right]$$

$$e_{k\alpha} = \frac{\rho_0}{\omega_{\alpha}^2 - r^2} \quad [2.23]$$

The resulting Hamiltonian is obtained after straightforward but tedious effort:

$$H = H_2 + H_3 \quad ,$$

$$H_2 = \sum_{\alpha, k} \omega_{\alpha}(k) J_{k\alpha} \quad ,$$

$$H_3 = \sum_{k, \ell, m} (J_k J_{\ell} J_m)^{1/2} \{ \delta_{k-\ell-m} \Gamma_1(k; \ell, m) \exp[i(\theta_k - \theta_{\ell} - \theta_m)] \\ + \delta_{k+\ell+m} \Gamma_2(k, \ell, m) \exp[i(\theta_k + \theta_{\ell} + \theta_m)] \}$$

+ c.c.

[2.25]

---

\*See ref. (5), pp. 296-323

(The coefficients  $\Gamma_1$  and  $\Gamma_2$  are given in the Appendix.)

To simplify notation in  $H_3$  we have written  $k$  for the index pair  $(\underline{k}, \alpha)$ , etc.

The equations governing the evolution of the internal wave field are Hamilton's equations:

$$\dot{\underline{j}}_{\underline{k}\alpha} = - \frac{\partial H}{\partial \underline{\theta}_{\underline{k}\alpha}} \quad , \quad \dot{\underline{\theta}}_{\underline{k}\alpha} = \frac{\partial H}{\partial \underline{j}_{\underline{k}\alpha}} \quad . \quad [2.26]$$

For linear waves, corresponding to neglect of  $H_3$ , we have

$$\dot{\underline{j}}_{\underline{k}\alpha} = 0 \quad , \quad \dot{\underline{\theta}}_{\underline{k}\alpha} = \omega_{\alpha}(k) \quad . \quad [2.27]$$

The term  $H_3$  in  $H$  describes the effect of all interacting triads of waves which satisfy the wavenumber conservation restrictions  $\underline{k} - \underline{l} - \underline{m} = 0$  or  $\underline{k} + \underline{l} + \underline{m} = 0$ , and allows for transfer of energy between members of the triad. Since  $H_3$  is assumed small compared with  $H_2$ , equation [2.27] indicates that the terms involving  $\Gamma_2$  are rapidly oscillating on the time scale of energy transfer among the modes. We shall henceforth neglect these terms, setting  $\Gamma_2 = 0$  in the numerical experiments to be described later in this paper. A similar argument applied to the  $\Gamma_1$  terms suggests that only those wave triads for which

$$\Delta \equiv \omega_{\alpha}(k) - \omega_{\beta}(l) - \omega_{\gamma}(m) \approx 0 \quad [2.28]$$

will have dynamical significance in our studies.

We shall refer to [2.28] as a "resonance condition." Those terms in  $H_3$  for which the resonance condition is not met can be transformed away by a sequence of canonical transformations. The resulting Hamiltonian has the form

$$H_1 = \bar{H}_2 + \bar{H}_3$$

where  $\bar{H}_2$  is a function of the transformed action variables and  $\bar{H}_3$  contains only wave-wave interactions for which the resonance condition [2.28] obtains.

For our present purposes we shall assume that those triads not satisfying the resonance condition may be neglected. How large the resonance mismatch  $\Delta$  must be for a triad to be neglected is, of course, a question that must be answered quantitatively. We shall return to this point in Section 4.

Another set of convenient variables are the dimensionless action-amplitude variables<sup>†</sup>

$$a_{\underline{k}\alpha} = (kB) \left( \frac{N_0}{\omega_\alpha} \right)^{1/2} \left[ \frac{2J_{\underline{k}\alpha}}{e_{\underline{k}\alpha} (BN_0)^3} \right]^{1/2} e^{-i\theta_{\underline{k}\alpha}} . \quad [2.29]$$

They are related to the original Fourier coefficients  $A_{\underline{k}\alpha}$  by

$$A_{\underline{k}\alpha} = i \frac{N_0 \sqrt{B}}{2k} [a_{\underline{k}\alpha} - a_{-\underline{k}\alpha}^*] . \quad [2.30]$$

---

<sup>†</sup>  $N_0$  and  $B$  are constant quantities having dimensions of frequency and length respectively. They may be considered as scale parameters of the Väisälä profile  $N(z)$ .

In the linear approximation,  $a_{k\alpha}$  represents the amplitude of a traveling plane wave having wave number  $k$  and mode number  $\alpha$ . It is normalized to describe the wave slope amplitude.

The equations of motion in terms of the  $a_{k\alpha}$  are

$$\begin{aligned} \dot{a}_{k\alpha} &= (a_{k\alpha}, H) \\ &= -2i \left( \frac{\omega_\alpha^2 - f^2}{\omega_\alpha} \right) \left( \frac{(kB)^2}{\rho_0 N_0^2 B^3} \right) \frac{\partial H}{\partial a_{k\alpha}^*} \end{aligned} \quad [2.31]$$

Here  $(a, H)$  represents the Poisson bracket of  $a$  with  $H$ . The explicit form of equation [2.31] as obtained from [2.25] is

$$\begin{aligned} \dot{a}_k + i\omega_\alpha a_k &= \sum_{\ell m} [\delta_{k+\ell-m} G_m^{k\ell} a_\ell^* a_m \\ &+ \delta_{k-\ell-m} G_{\ell m}^k a_\ell a_m] \end{aligned} \quad [2.32]$$

The coefficients  $G$  are expressed in the Appendix as functions of  $\Gamma_1$ .

In this equation there are two types of interaction terms. These are denoted sum and difference interactions according to the wavenumber conservation relations  $k=m+\ell$  respectively.

### 3. Test Wave Model

To provide a simple model for preliminary study we introduce the test wave system. Here a single  $(k, \alpha)$  mode, identified as the test wave, is permitted to interact with an ambient field consisting of the remaining modes. However the ambient modes are not allowed to interact among themselves. Test wave models are often employed for calculating relaxation rates in transport theory, where standard approximation schemes in statistical mechanics may be applied. Numerical integration of equations such as [2.26] can be used to evaluate the validity of these approximation methods. Later papers in this series will study this problem in detail.

We can also use the test wave model to test whether a particular background wave amplitude spectrum is an equilibrium spectrum with respect to the dynamics. If it is, the mean action of the test wave (averaged over ambient initial conditions) must decay to its equilibrium value.

Our system consists of  $2M+1$  waves formed in  $M$  triads. We let  $k$  designate the test wave mode  $(k, \alpha)$  and  $\ell, m$  designate ambient wave pairs  $(\ell, \beta), (m, \gamma)$  respectively. The appropriate equations of motion are then

$$\begin{aligned}
 \text{TEST WAVE: } \quad \dot{a}_k + i\omega_\alpha a_k &= \sum_{\ell m} \left[ \delta_{k-\ell-m} G_{\ell m}^k a_\ell a_m + \delta_{k+\ell-m} G_m^{k\ell} a_\ell^* a_m \right] \\
 \text{BACKGROUND: } \quad \dot{a}_\ell + i\omega_\beta a_\ell &= \delta_{\ell-k-m} 2G_{km}^\ell a_k a_m + \delta_{\ell-k+m} G_k^{\ell m} a_k^* a_m \\
 &+ \delta_{\ell+k-m} G_m^{\ell k} a_k^* a_m .
 \end{aligned}
 \tag{3.2}$$



It is easily verified that [3.2] admits  $M+1$  conservation laws.\*

In our computations, initial conditions for the ambient modes are chosen from a Gaussian distribution for the action-amplitudes.

$$P(a_{k\alpha}) = \frac{1}{2\pi\sigma_{k\alpha}} \exp[-|a_{k\alpha}|^2/2\sigma_{k\alpha}] \quad [3.3]$$

Thus, the initial wave phases are chosen from a distribution uniform in  $-\pi, \pi$ . Averages over ambient initial conditions with distribution [3.3] will be denoted  $\langle \rangle$ . The mean square action amplitude  $\sigma_{k\alpha}$  is related to the power density spectrum for the vertical displacement

$$\langle \xi_3^2 \rangle = \int_{\alpha=1}^{\infty} \int d^2k \psi(k, \alpha); \quad [3.4]$$

$$\langle |a_{k\alpha}|^2 \rangle = \sigma_{k\alpha} = 2k^2 \left( \frac{4\pi^2}{\Sigma_0} \right) \psi(k, \alpha) \quad [3.5]$$

Equivalently, the mean wave action (see equation [2.29]) is given by

$$\langle J_{k\alpha} \rangle = \frac{\rho_0 N_0^2 B \omega_\alpha(k)}{\omega_\alpha^2(k) - f^2} \left( \frac{4\pi^2}{\Sigma_0} \right) \psi(k, \alpha) \quad [3.6]$$

The specific  $\psi(k, \alpha)$  used for this study was the Garrett-Munk "75+" spectrum (17), an experimentally derived spectrum for internal waves which appears to be an equilibrium spectrum for the ocean.

---

\*See J. D. Meiss and K. M. Watson, ref. (5), pp. 296-323.

#### 4. Numerical Methods and Results

Our emphasis in this section will be on computational techniques and qualitative features of solutions. Detailed application to the ocean will be published separately.

We represent the continuous wave system with a finite number  $(2M+1)$  of waves. Each wave must correspond to a wavelength which "fits" into the (assumed) square area  $\Sigma_0$ . This implies a base grid in wavenumber space with grid spacing

$$\Delta k_x = \Delta k_y = \frac{2\pi}{\sqrt{\Sigma_0}} \quad . \quad [4.1]$$

Since the test wave wavenumber  $k$  is fixed (given), the wavenumber conservation equations

$$\underline{k} = \underline{m} + \underline{l} \quad [4.2]$$

imply that a single grid can act as coordinate system. For example, choosing the  $x$ -axis along  $\underline{k}$ , each point  $(m_x, m_y)$  defines a triad as shown in Figure 1. As discussed in Section 2, the most important triads for energy transfer are expected to be those for which the resonance condition  $\Delta \equiv \omega_\alpha + \omega_\beta - \omega_\gamma \approx 0$  holds. For a given set of modenumbers  $\alpha, \beta, \gamma$  and a given resonance mismatch  $\Delta$ , each resonance condition defines a curve in the  $m_x, m_y$  plane. Examples of curves for various  $\Delta$  are shown in Figure 1. Our procedure will be to include those triads which lie on grid points for which  $|\Delta| \leq \Delta_{\max}$ . For a given computation the parameters

$\Delta k$  and  $\Delta_{\max}$  must be obtained empirically. Before discussing this further we present a sample computation of the full system of equation to illustrate the general character of the solution.

Figure 2 displays a typical example of the mean test wave action for the ocean internal wave system. The frequency and modenumber of the test wave are  $\omega_{\alpha} = 7f$  and  $\alpha = 4$ , respectively. We include the first nine WKB vertical modes of the ambient spectrum. This corresponds to including fifteen resonance curves in the calculation. The magnitude of the initial test wave action-amplitude is chosen to be  $0.1 \sqrt{\sigma_{k\alpha}}$  and the corresponding initial phase is fixed arbitrarily. The ambient initial conditions are picked with a random number generator according to the distribution [3.4]. To integrate the equation of motion [3.2], we use a variable step size, variable order Adams integration scheme (20). The test wave action is averaged over  $I=100$  ambient realizations, integrating to  $t=1000/N_0$  for each. The entire computation required approximately 7 minutes C.P. time on a CDC 7600 computer. The salient features of Figure 2 are a rapid rise of the test wave action by a factor of 100 in the first 20 time units, followed by small oscillations about a value slightly larger than its expected (Garrett-Munk) equilibrium value (indicated by the dotted horizontal line). We have found that these fluctuations decrease with increasing  $I$ , and that the mean value is constant upon variation of the initial test wave amplitude providing this amplitude is small ( $\leq 0.25 \sqrt{\sigma_{k\alpha}}$ ).

The effect of choosing different values of  $\Delta k$  and  $\Delta_{\max}$  is best illustrated by a simple model calculation. For the remainder of this section we keep only the sum interactions in [3.2] and arbitrarily set the coupling coefficients

to  $G_{\ell m}^k = G_k^{\ell m*} = G_k^{m \ell*} = G \equiv \frac{1}{2} (-1+i)$ , ignoring the complicated wavenumber and frequency dependence of the real ocean.

To investigate the effect of off-resonant triads we consider 25 triads, 13 with  $\Delta=0$  and 12 with  $\Delta=\Delta_{\max}$ . Figures 3 and 4 present plots of the short time behavior of the mean action for various  $\Delta_{\max}$ . In Figure 3 the phases of the ambient modes at  $t=0$  are chosen so that the initial growth rate of the test wave action is maximal. That is, the sum of the phases of the background waves in [3.2] plus the phase of  $G$  is zero. It is known that this set of initial conditions results in "square wave" phase oscillations and maximum coupling of the interacting waves (21). These coherent solutions in Figure 3 show that the effect of off-resonant triads is to produce oscillations about the growth rates of the resonant triads. For  $t \ll 1/\Delta_{\max}$  the growth rate is essentially given by the  $\Delta_{\max}=0$  curve.

For later times the action oscillates about the  $\Delta_{\max}=\infty$  curve (where in effect only 13 resonant triads are kept, all with  $\Delta=0$ ). The frequency of these oscillations depends linearly on  $\Delta_{\max}$ .

In Figure 4 the initial phases are chosen randomly. From [3.2] we see that the initial growth rate of the mean action is zero. For later times, the growth rate (calculated as an average over 100 ambient initial conditions) is about one half of the maximal rate. As  $\Delta_{\max}$  is increased, the growth rate decreases as in Figure 3, but now the oscillations are washed out by the phase averages. The ambient phases do not remain completely random for  $t>0$ : If we make the random phase approximation using the Krylov-Bogoliubov-Mitropolsky (14) (KBM) perturbation theory to obtain

an estimate for the growth rate, we get a rate that is less than that of the dynamical calculation. The KBM and maximal rates represent extremes, the first implying complete incoherence while the latter implies complete coherence. We plan to quantify the significance of phase coherence in a later paper.

As a final model, more closely related to the full ocean calculation, we include only triads with modenumbers  $\alpha=4$ ,  $\beta=6$  and  $\gamma=2$  corresponding to the resonance curves of Figure 1. Again we choose the  $G$ 's to be equal. With this model we can discuss the effect of both  $\Delta k$  and  $\Delta_{\max}$  on the growth rate. For this purpose we tentatively assume that the test wave relaxes exponentially to equilibrium. This type of relaxation would be predicted by a Langevin model for the system. To provide a rough estimate for the growth rate,  $\nu$ , we calculate the time,  $t_{1/2}$ , required for the test wave to grow to half of its equilibrium value. Then  $\nu = -\log 2 / t_{1/2}$ . The exponential relaxation assumption is clearly not valid for very short times when  $\langle |a_{k\alpha}|^2 \rangle$  grows as  $t^2$  (since the ambient phases are initially random). For longer times the oscillations caused by non-resonant triads must also provide an error in the fit. However for the purpose of investigating the effects of changing  $\Delta k$  and  $\Delta_{\max}$  our measure is sufficient.

In Figure 5 we plot  $\nu$  as a function of  $\Delta_{\max}$  for various values of  $\Delta k$ . These curves approach  $\nu \approx .02N_0$  for  $\Delta_{\max} \gtrsim .1N_0$  independently of  $\Delta k$ . Since varying  $\Delta k$  changes the number of triads within a given resonance width, we see that keeping a small number of triads is sufficient to obtain a good estimate of  $\nu$ . For example, the value of  $\nu$  for  $\Delta_{\max} = .1$

and  $\Delta k = .27$  (14 triads) differs by only 15% from that with  $\Delta k = .10$  (93 triads). Varying the initial action between  $10^{-4} \sigma_{k\alpha}$  and  $.05 \sigma_{k\alpha}$  does not significantly change the growth rate or the final action. Further increase of the initial action changes the growth rates drastically indicating that the exponential assumption breaks down.

Figure 5 indicates that quantitative results may be obtained for  $\Delta_{\max} \approx 5\nu$ . Since  $\Delta_{\max}$  and  $\nu$  define the only available time scales, these quantities can be expected to scale together and produce reliable results if  $\Delta_{\max}$  is chosen, self consistently to be "a few times  $\nu$ ."

Finally, in Figure 6 we see that the time required for the test wave action to reach equilibrium does not depend strongly on  $\Delta_{\max}$ . Although initially the two curves grow at quite different rates [ $\nu(\Delta_{\max} = .03N_0) \approx 1.5 \nu(\Delta_{\max} = .2N_0)$ ], for later times the curves grow at similar rates and reach their equilibrium values at comparable times.

Acknowledgments

This research was partially supported by the Office of Naval Research under contract N00014-78-C-0050. The authors wish to express appreciation to Lawrence Berkeley Laboratory for the use of their computing facilities and to N. Pereira and P. Yau for helpful discussions.

Appendix

The coupling coefficients which appear in equations [2.25] and [2.32] of the main text are defined explicitly by the following set of equations:

$$\Gamma_2 = \rho_0 (32 \omega_\alpha \omega_\beta \omega_\gamma e_{k\alpha} e_{l\beta} e_{m\gamma})^{-1/2} [G(k;l,m) + G(l;m,k) + G(m;k,l)]/3, \quad [A.1]$$

$$\begin{aligned} G(k;l,m) = & (\omega_\beta^2 - \omega_\gamma^2) \frac{l \times m}{k^2} \cdot \frac{f}{\omega_\alpha} \left( \frac{\mu_{lm}^k}{k^2} - \frac{\nu_{klm}}{k^2 l^2 m^2} (l \cdot m) \right) \\ & + i(\omega_\alpha^2 - f^2) \left[ \left( \frac{\mu_{km}^l}{l^2} + \frac{\mu_{kl}^m}{m^2} \right) (l \cdot m) \right. \\ & \left. + \frac{\nu_{klm}}{k^2 l^2 m^2} \left( (l \cdot k)(k \cdot m) + (l \times m)^2 \frac{f^2}{\omega_\beta \omega_\gamma} \right) \right], \quad [A.2] \end{aligned}$$

$$\Gamma_1(k, \omega_\alpha; l, \omega_\beta, m, \omega_\gamma) = 3\Gamma_2(k, \omega_\alpha, -l, -\omega_\beta, -m, -\omega_\gamma), \quad [A.3]$$

$$\mu_{lm}^k \equiv \frac{1}{\rho_0} \int_{-H}^0 dz \rho W'_{k\alpha} W'_{l\beta} W'_{m\gamma}, \quad \nu_{klm} \equiv \frac{1}{\rho_0} \int_{-H}^0 dz \rho W'_{k\alpha} W'_{l\beta} W'_{m\gamma}, \quad [A.4]$$



$$G_m^{kl} = -i \frac{k}{lm} \sqrt{\frac{2\omega_\beta^\omega \gamma^e \ell \beta^e m \gamma}{\omega_\alpha^e k \alpha}} B^{1/2} N_0 \Gamma_1^*(m; k, \ell) . \quad [A.5]$$

$$G_{lm}^k = -\frac{i}{2} \frac{k}{lm} \sqrt{\frac{2\omega_\beta^\omega \gamma^e \ell \beta^e m \gamma}{\omega_\alpha^e k \alpha}} B^{1/2} N_0 \Gamma_1(k; \ell, m) . \quad [A.6]$$

References

1. Phillips, O. M. (1977), The Dynamics of the Upper Ocean, (Cambridge Univ. Press), Ch. 5, pp. 199-252.
2. Davidson, R. C. (1972), Methods in Nonlinear Plasma Theory, (Academic Press, New York), pp. 133-173.
3. Ford, J. (1973), Adv. in Chem. Phys. 24, 155-185
4. Scott, A. C., Chu, F. Y. F., and McLaughlin, D.W. (1973), Proc. IEEE 61, 1443-1483; the existence of internal solitary waves was shown by Benjamin, T. B. (1967), J. Fluid Mech. 29, 559-592 and Davis, R. E., and Acrivos, A. (1967), J. Fluid Mech. 29, 593-607.
5. Topics in Nonlinear Dynamics (1978), ed. S. Jorna, AIP Conf. Proc. No. 46 (AIP, New York).
6. Mazur, P. and Montroll, E. (1960), J. Math. Phys. 1, 70-84.
7. Ford, G., Kac, M. and Mazur, D. (1965), J. Math. Phys. 6, 504-515.
8. Cukier, R.I., Shuler, K. E. and Weeks, J. D. (1972), J. Stat. Phys. 5, 99-112.
9. Hasselmann, K. (1962), J. Fluid Mech. 12, 481-500; *ibid.* (1963) 15, 273-281; *ibid.* (1963) 15, 385-398; (1966) Rev. Geophys. 4, 1-32.
10. Snider, R. F. (1960), J. Chem. Phys. 32, 1051-1060.
11. Brout, R. and Prigogine, I. (1956), Physica 22, 621-636.
12. See, for example, Lax, M. (1966) Rev. Mod. Phys. 38, 541-566.
13. Bogoliubov, N. N. and Mitropolsky, Y. A. (1961), Asymptotic Methods in the Theory of Nonlinear Oscillations (Gordon and Breach Science Publ., New York).
14. Case, K. M. (1966) Prog. Theor. Phys., Suppl. No. 37, 1-20.
15. McComas, C. H. and Bretherton, F. P. (1977) J. Geophys. Res. 82, 1397-1412.
16. Olbers, D. J. (1976), J. Fluid Mech. 74, 375-399.
17. Garrett, C. J. R. and Munk, W. H. (1972), Geophys. Fluid Dyn. 2, 225-264; (1975) J. Geophys. Res. 80, 291-297.
18. Garrett, C. J. R. and Munk, W. H. (1979) Annual Rev. of Fluid Mech. (in press).

19. This Lagrangian is discussed by Bretherton, F. P. and Garrett, C. J. R. (1969), Proc. Roy. Soc. A302, 529-554; McComas and Bretherton (ref. 15) use Lagrange's equations for their discussion.
20. Hindemarsch, A. C. and Byrne, G. D. (1976) in Numerical Methods for Differential Systems, eds. Lapidus, L. and Scheisser, W. E., (Academic Press, New York), pp. 147-166.
21. Meiss, J. D. (1979) "On the Integrability of Multiple Three Wave Interactions," (to be published in Phys. Rev.).

Figure Captions

- Figure 1. Resonance curves for sum interaction using the deep ocean dispersion relation:  $\omega_{\alpha}^2(k) = f^2 + [kBN_0/\pi(\alpha-k)]^2$ . For these curves  $\alpha = 4$ ,  $\beta = 6$ ,  $\gamma = 2$ ,  $\omega_{\alpha}(k) = 7f$ . Arrowed is a typical wavenumber triad.
- Figure 2. Mean test wave action as a function of time with 91 triads on 15 resonance curves and coupling coefficients for the deep ocean.  $\alpha = 4$ ,  $\omega_{\alpha} = 7f$  and the mean is taken over  $I = 100$  initial conditions.
- Figure 3. Mean test wave action for the two-row model. The ambient initial phases are fixed to give maximum initial growth rates.  $I = 100$ .
- Figure 4. Mean test wave action for the two-row model. Ambient initial phases are chosen randomly for the dashed curves. Curves labeled "maximal" are from Figure 3. The KBM curve assumes the random phase approximation.
- Figure 5. Growth rate,  $\nu$ , as a function of  $\Delta_{\max}$  and  $\Delta k$  for the single resonance curve model.
- Figure 6. Mean test wave action for the single resonance model. For  $t \leq 100/N_0$  the  $\Delta_{\max}$  solution grows faster than the  $\Delta_{\max} = .03$  solution. For longer times (right scale) evolution is at a similar rate.

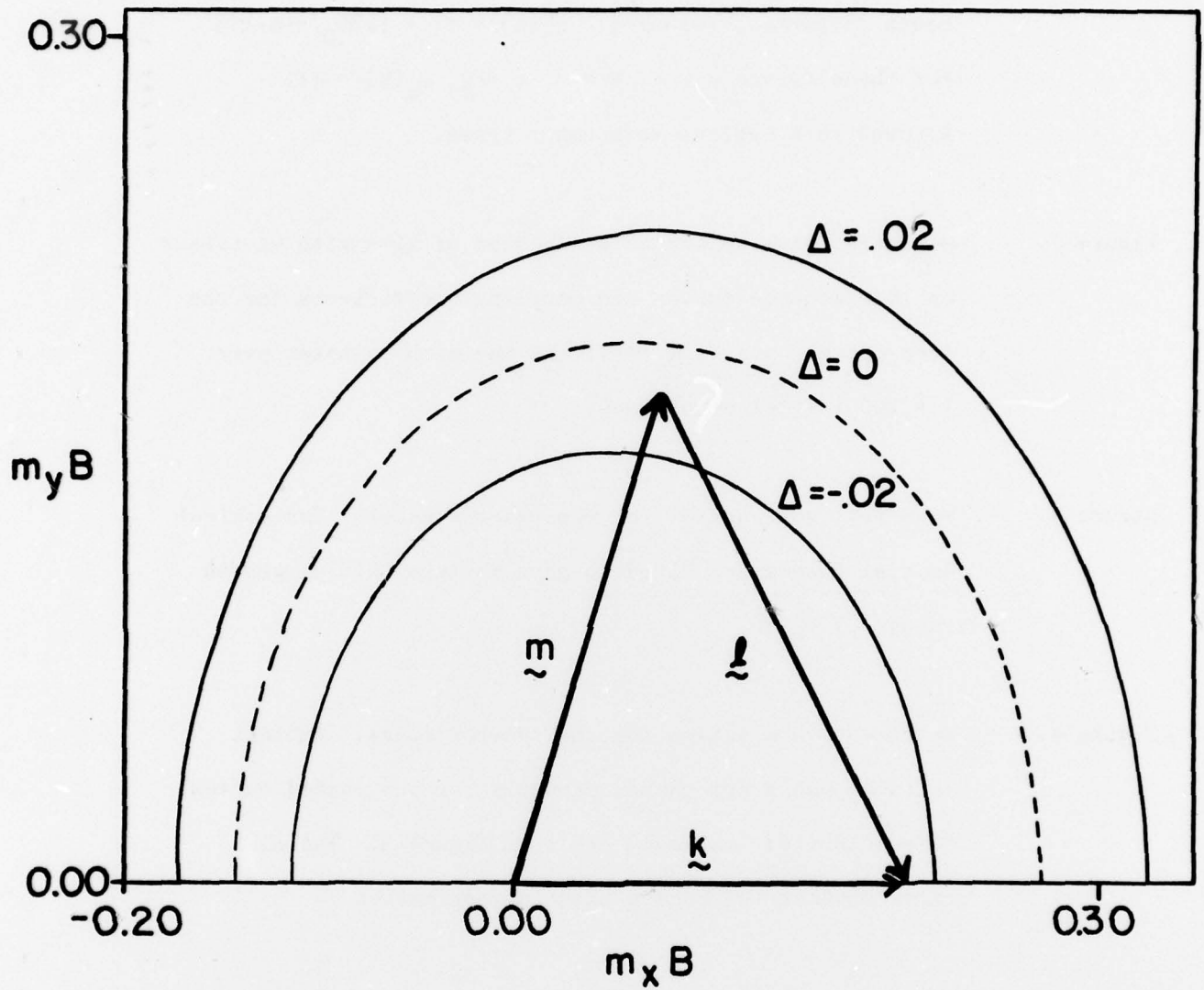


Figure 1

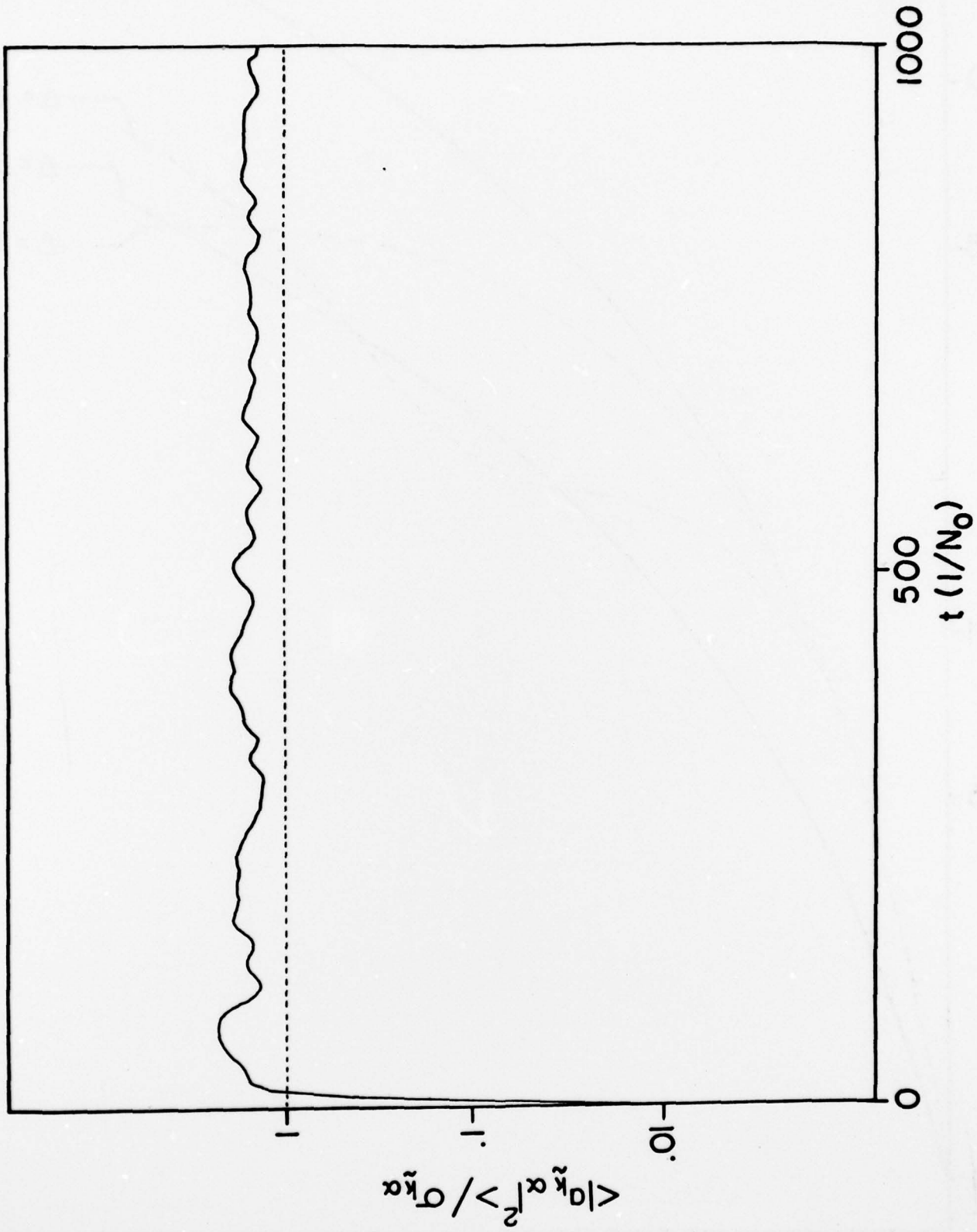


Figure 2

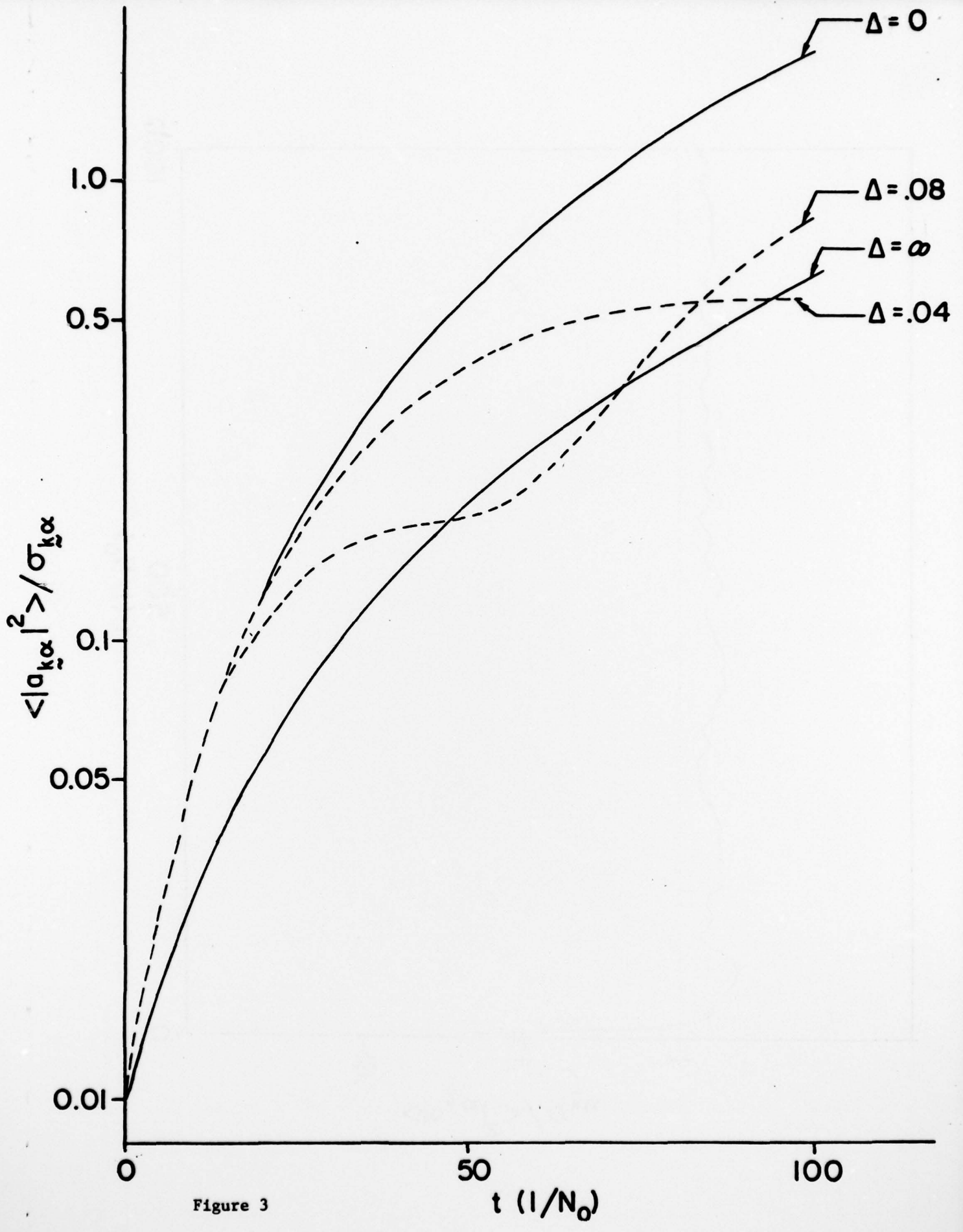


Figure 3

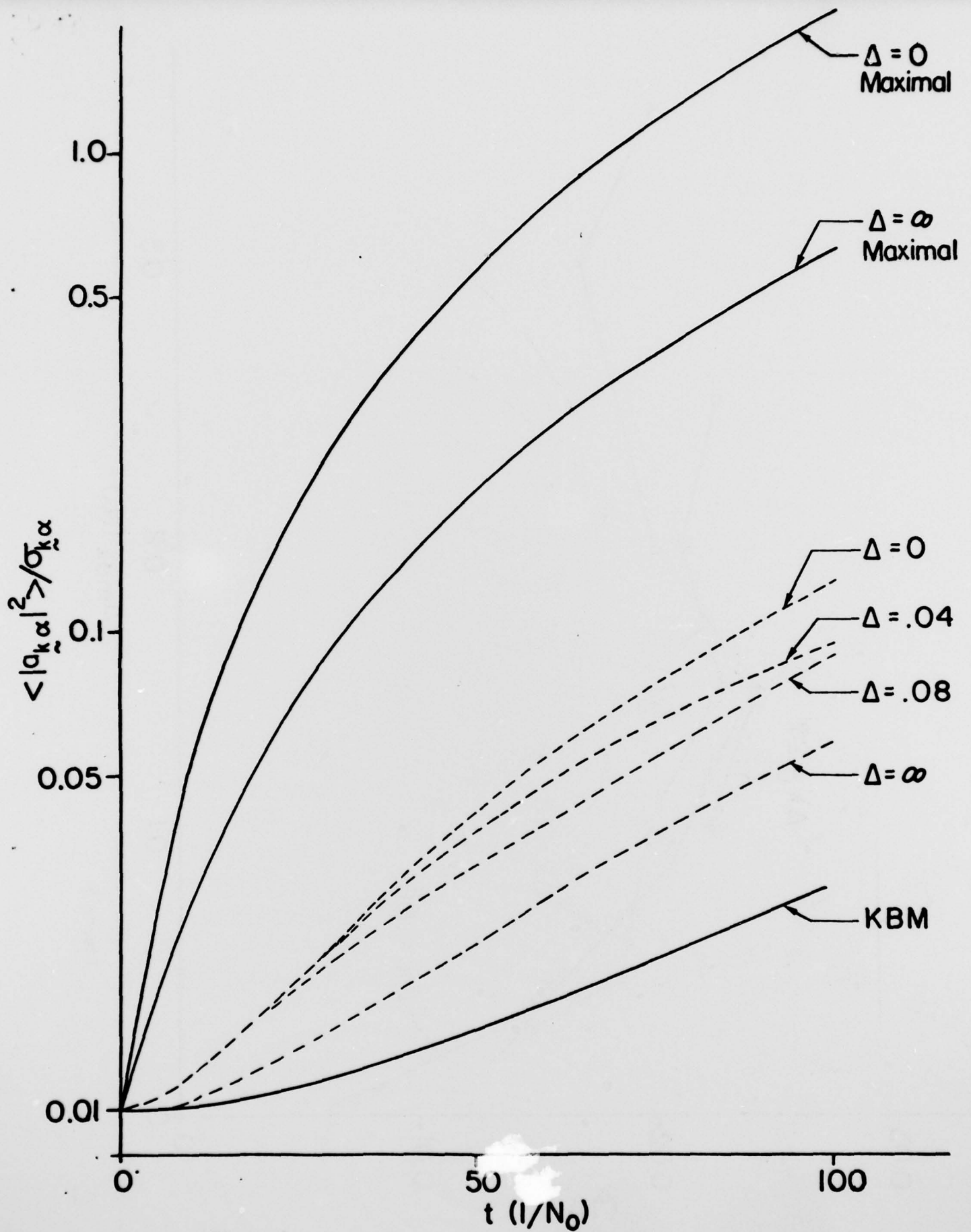


Figure 4



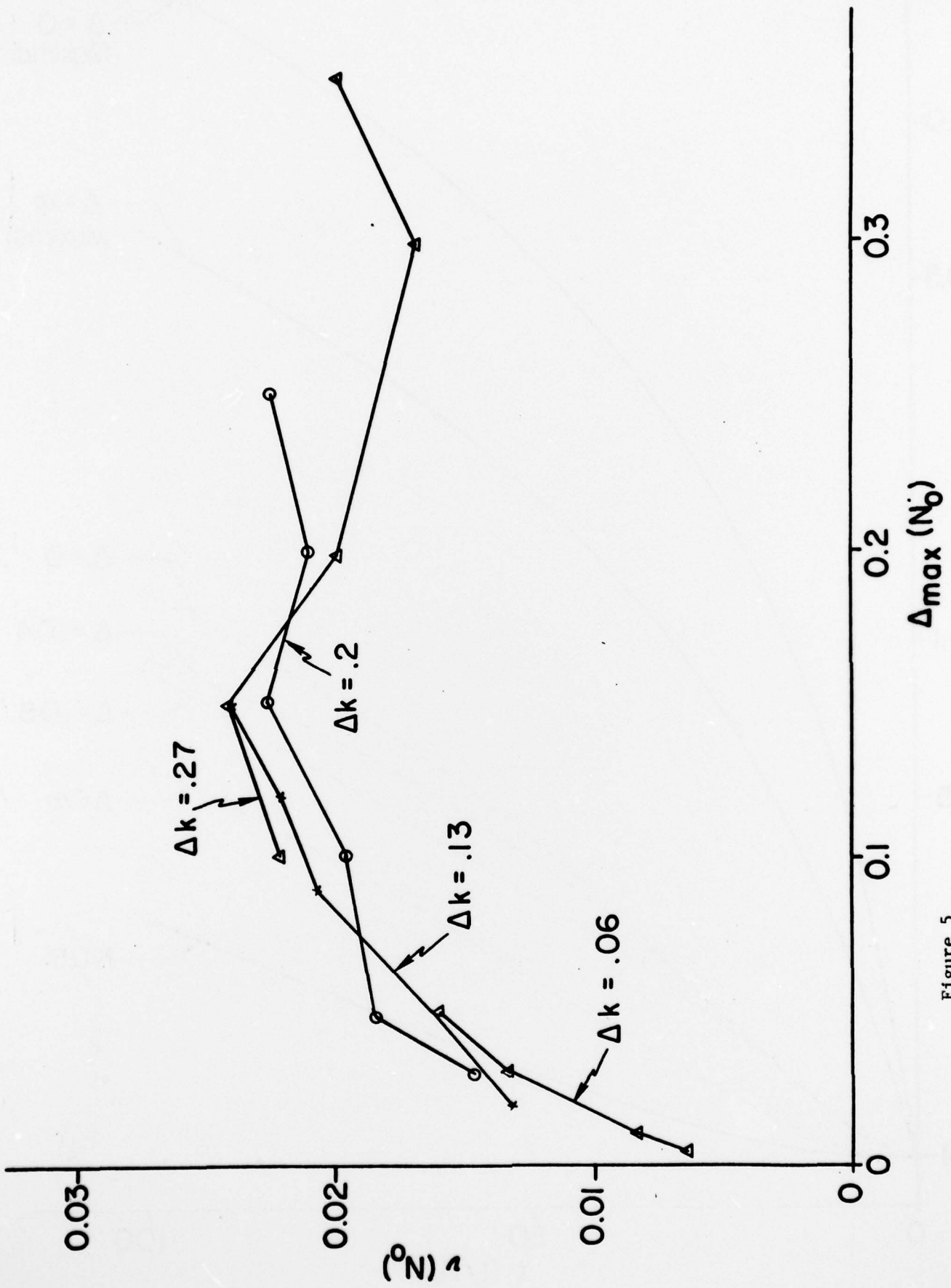


Figure 5

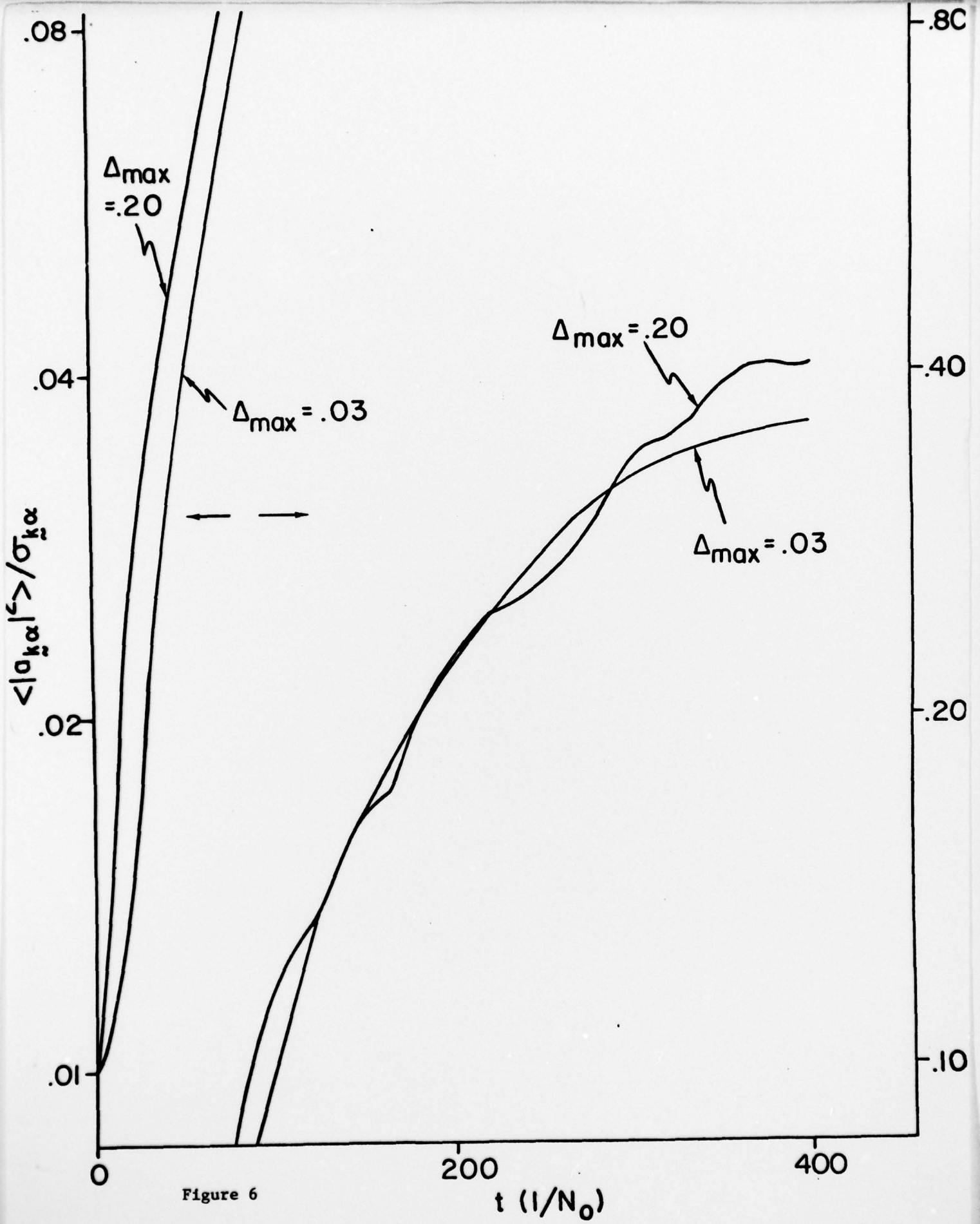


Figure 6